Theoretical analysis of directly modulated optical OFDM signals over an IM/DD fiber link

Christian Sánchez Costa, Beatriz Ortega Tamarit and José Capmany Francoy

Instituto de Telecomunicaciones y Aplicaciones Multimedia,
Universitat Politècnica de València,
8G Building - access D - Camino de Vera s/n - 46022 Valencia (Spain)
Corresponding author: bortega@iteam.upv.es

Abstract

In this paper we present the intensive theoretical labor carried out to describe optical communication systems which employ orthogonal frequency division multiplexing (OFDM), and, more concretely, those systems which use direct laser intensity modulation and direct detection. Firstly, we propose an analytical model to study in detail the main phenomena which affect the signal information detected at the receiver. Moreover, the analytical model is complemented with a study of signal clipping at the transmitter and the filtering effects affecting the signal through the communication system. With the analytical model reported we can describe in a rather comprehensive way the main phenomena as well as exploring and optimizing the final system performance of OOFDM systems with direct modulation and detection.

By taking advantage of the analytical model derived, we propose a pre-distortion technique which improves the modulation efficiency, making possible to increase the signal information term without increasing the nonlinear distortion at the receiver, improving in this way the system performance obtained. An alternative technique for the system performance improvement based on optical filtering is also mathematically studied in order to understand exactly its working principle, the improvement obtained, as well as its potentiality. The derived mathematical expressions allows us to systematically explore the different effects involved in the final performance obtained, the study of OOFDM systems with different optical filtering structures, as well as the possibility of optimization in a quick and efficient manner different optical filtering structures.

1. Introduction

OFDM is a multi-carrier format widespread used in wireless communications and DSL applications [1,2]. Since 2005 optical OFDM has also attracted lots of attention for a great variety of optical communication scenarios, from long-reach to short-reach optical links, or communications systems based on single mode, multimode and plastic optical fiber [3-5]. In the context of access networks, passive optical networks have emerged as a coste-fficient architecture to provide advanced and speed rate demanding communications applications. In this cost-sensitive scenario, OOFDM is a promising format/multiplexing technique, what has led to a high number of research results published by several investigation groups [6,7]. Besides its versatility, the potentials of OOFDM have contributed as well to this interest: it can offer high spectral efficiencies by using high quadrature-amplitude modulation formats, robustness to frequency roll-off of transceiver electronics, dispersion equalization complexity easily scalable with transmission rate or subcarrier granularity. The proposed transceiver architecture varies for each scenario depending on the required trade-off between system performance/cost. When the optical intensity is used for information transmission, a simple pin photodetector is appropriate for the opto-electronic conversion to recover the transmitted information, what is called intensity modulated/directly detected (IM/DD) system. This variant is more appropriate for medium and short reach applications where the cost is of great concern, such as metro and access optical networks. The direct modulation of a laser in the OFDM transmitter brings additional advantages in terms of cost reduction, compactness, low power consumption and high optical output power.

The direct modulation of a laser in the OFDM transmitter brings additional advantages in terms of cost reduction, compactness, low power consumption and high optical output power.

Nevertheless, its performance is severely limited by distortions arising from the laser and photodetector nonlinearities and the propagation of the chirped signal through the dispersive link connecting the central office and the optical network unit. Analytical models which enlighten the physics behind the performance of directly modulated/detected (DM/DD) OOFDM systems can be of great help for their design and the proposal of techniques aimed to increase the performance obtained. Previous published analytical models focus on the influence of the transceiver electronics design parameters but not on the direct modulation process and fiber transmission effects [8], or are based on not general mathematical assumptions [9,10]. In this sense, we present a theoretical analysis using a detailed mathematical treatment to study the effects of the laser nonlinearity and the global impact of the laser chirp and chromatic dispersion with regard to the system performance. Moreover, a comprehensive framework for the quick, systematic and efficient evaluation of DM/DD OOFDM systems is proposed after i) simplifying the expressions describing the linear effects and the second order intermodulation distortion in DM/DD OOFDM systems, ii) the study of the effects of linear filtering through the communication system causing inter-carrier and inter-symbol interferences (ISI and ICI), and iii) the study of the effects of signal clipping at the transmitter.

In order to overcome the underlying limiting system performance in IM/DD OOFDM systems, such as the nonlinear distortion, several solutions have been proposed in order to overcome it (e.g., [11,12]). Our proposal is based on the employment of pre-distortion at the transmitter and in the frequency domain (before the transmitter inverse Fourier transform), and makes use of the analytical model previously reported for the reconstruction of the interference. Unlike previous references about digital pre-distortion, the technique here proposed aims to mitigate the nonlinear distortion with an end-to-end perspective, rather than only that originated by the optical modulator.
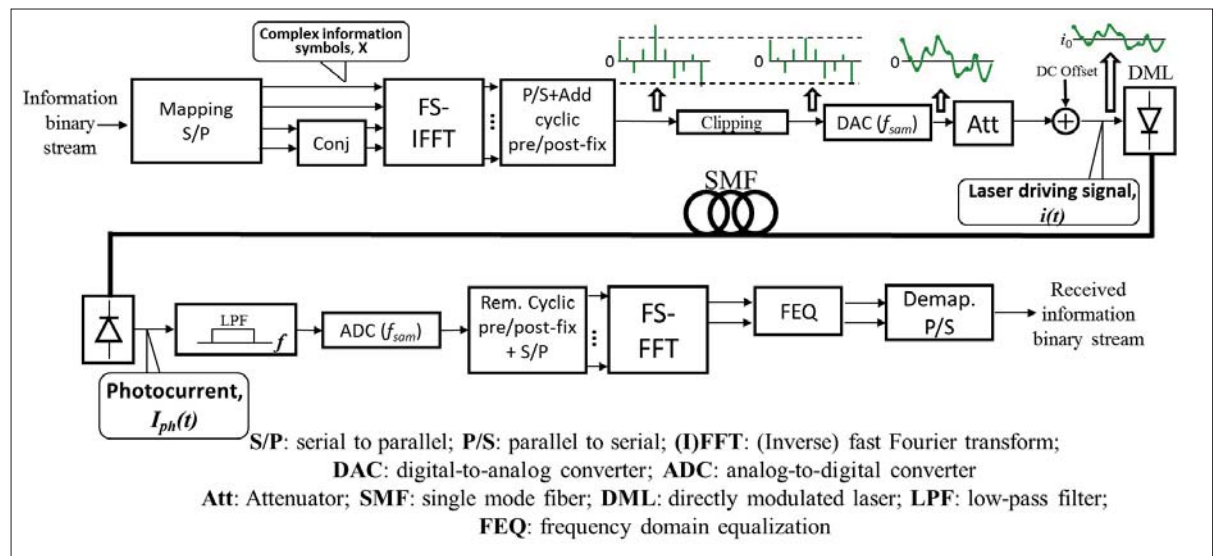
The employment of an optical filter to improve the system performance by suitable conversion of the inherent frequency modulation at the laser transmitter output into additional intensity modulation at the end of the link has been studied for traditional modulation formats [13], and recent results showed considerable power budget improvements for DM/DD OOFDM systems [14]. Nevertheless, this approach is only qualitatively understood in previous literature and further work is necessary to grasp the theoretical foundations which can provide the design criteria for optimum operation. By extending the previously presented theory, we provide an end-to-end analytical model to describe the operation of a DM/DD OOFDM system when an arbitrary optical filter is inserted in the dispersive link.

2. Analytical modelling

2.1. System description
The optical OFDM communication system is basically composed of an OFDM transmitter, the directly modulated laser (DML), the dispersive fiber link, a photodetection stage, and, finally, the OFDM receiver, as depicted in Fig. 1.

In the OOFDM system, the information binary data is mapped into M-QAM complex symbols and a block of the resulting complex symbols is fed to an Inverse Fast Fourier Transform (IFFT) processor with a size equals to FS.

■ **Figure 1.** Schematic illustration of the DM/DD OOFDM system.

$$x[n] = \sum_{k=0}^{FS-1} X_k \cdot exp\left(j \cdot 2\pi \cdot k \frac{n}{FS}\right), \quad n = 0,1,...FS-1 \quad (1)$$

In order to obtain a real-valued signal $x[n]$ at the output, the original information complex symbols and their corresponding conjugate values are arranged with Hermitian symmetry at the IFFT input. The obtained real-valued discrete signal is composed of N subcarriers, each of them modulated by an information complex symbol. Note that some symbols X_k at highest frequencies may be set to zero in order to introduce oversampling. After parallel-to-serial conversion, a cyclic pre/post-fix is added to each OFDM symbol in order to combat ISI and ICI effects, and hard clipping in the digital domain is applied in order to limit the amplitude swing of the OFDM signal. Finally, the signal is interpolated and low-pass filtered. The OFDM symbol starting at $t=0$ and with duration T can be expressed as:

$$s(t) = \sum_{k=1}^{N} |X_k| \cdot cos\left(\Omega_k t + \varphi_{X_k}\right) * h_{trx}(t) \quad (2)$$

where $X_k = |X_k| \, exp(j \, \varphi_{Xk})$ are the information complex symbols, Ω_k is the angular frequency of the is the kth OFDM subcarrier, and $h_{trx}(t)$ is the impulse response of the transmitter. The value of the discrete frequency Ω_k is given by $k \cdot \Delta\Omega$, where $\Delta\Omega$ is the spacing angular frequency between consecutive subcarriers. The spacing angular frequency $\Delta\Omega$ is given by 1/T, where $T=FS \cdot f_{sam}$ and f_{sam} is the sampling rate. The analog OFDM signal is then scaled by a factor to yield a certain value of peak current and a dc value is added to operate the optical source. The input current to the laser is then given by:

$$i(t) = i_0 + i_m(t) = i_0 + \sum_{k=1}^{N} 2 \cdot i_k \cdot cos\left(\Omega_k t + \varphi_{X_k}\right) * h_{trx}(t) \quad (3)$$

where i_0 represents the dc-offset added just before the laser, m is the scaling factor determined by the electrical attenuation to operate the laser within a certain region ($|i_m(t)|<\Delta i$), and $i_k \cdot exp((-)j\varphi i\_k)$ is the driving current coefficient at frequency $(-)\Omega_k$. In the case that the electrical filter htrx does not affect the signal band, the intensity coefficient i_k is equal to $m/2 \cdot |X_k|$. The OFDM symbol current is fed into the laser to modulate the optical intensity, whose process is governed by the following system of equations [15]:

$$\frac{\partial p(t)}{\partial t} = \left[\Gamma \cdot v_g \cdot a_g \frac{n(t)-n_t}{1+\varepsilon_{nl} \cdot p(t)} - \frac{1}{\tau_p}\right] p(t) + \zeta \Gamma B \cdot n^2(t) \quad (4.1)$$

$$\frac{\partial n(t)}{\partial t} = \frac{i(t)}{e \cdot V} - A \cdot n - B \cdot n^2 - C \cdot n^3 - v_g \cdot a_g \frac{n(t)-n_t}{1+\varepsilon_{nl} \cdot p(t)} \cdot p(t) \quad (4.2)$$

$$\frac{\partial \phi(t)}{\partial t} = \frac{1}{2}\alpha \cdot \Gamma \cdot v_g \cdot a_g(n(t) - n_t) \quad (4.3)$$

where $p(t)$, $n(t)$ are the photon and carrier densities in the laser active region, respectively, $\phi(t)$ is the phase of the output optical signal, Γ is the confinement factor, v_g is the group velocity, ag is the linear material gain coefficient, n_t is the transparency carrier density, ε_{nl} is the nonlinear gain coefficient, τ_p is the photon lifetime, ζ

determines the fraction of spontaneous emission that is emitted into the fundamental mode of the laser, V is the volume of the active region, $i(t)$ is the driving current fed into the laser, e is the electron charge, A is the non-radiative recombination coefficient, B is the radiative-recombination coefficient and C is the Auger recombination coefficient.

The optical fiber is considered as a linear medium, whose transfer function is given by:

$$H(\omega) = exp(j \cdot \beta(\omega)L) = exp(j \cdot (\beta_0 + \beta_1(\omega - \omega_0) + \beta_2(\omega - \omega_0)^2)L) \quad (5)$$

where $\beta(\omega)$ is the propagation constant of the fiber, β_0 its value at $\omega = \omega_0$, β_1 and β_2 are its first and second derivatives evaluated at ω_0 and L is the length of the fiber. β_2 is related to the dispersion parameter D of the fiber through $\beta_2 = -D\lambda_0^2/(2c)$ where λ_0 is the laser emission wavelength and c is the speed of light in vacuum.

Once the optical signal is propagated through the fiber, the optical intensity is detected by means of a square-law photodetector:

$$I_{ph}(t) = R|E(t, z = 0)|^2 \quad (6)$$

where R is the responsivity of the photodetector. The OFDM signal processing performed at the receiver is essentially the inverse of that described for the transmitter. After calculating the FFT of the received time domain signal, the complex symbols are equalized and demapped to bits in order to generate the received information binary stream.

2.2. Mathematical formulation
2.2.1. Study of the optical effects in DM/DD OOFDM systems

Our goal is to obtain a mathematical expression of Eq. (6), since it is a much more useful tool for the understanding of directly modulated OOFDM systems than the observation of the final results in numerical simulations. Neglecting transmitter filtering effects and assuming infinitely extended RF-waves in Eq. (3), the first step is the derivation of a suitable mathematical expression for the signal at the laser output. For such goal, a perturbative analysis of Eqs. (4.1)-(4.3) is performed [19], which renders the first and second order optical intensity versus driving current transfer functions, $H_{p1}(\omega_k)$, $H_{p2}(\omega_k)$, $H_{p1}(\omega_k,\omega_1)$, as well as the first and second order optical phase versus driving current transfer functions $H_{\phi1}(\omega_k)$, $H_{\phi2}(\omega_k)$, $H_{\phi1}(\omega_k,\omega_1)$. The complex electric field amplitude at the laser output can be then approximated by:

$$E(t, z = 0) = \sqrt{P_0 + P_1(t) + P_2(t) + P_{11}(t)}$$
$$exp(j \cdot \sum_{k=1}^{N} m_k sin(\Omega_k t + \varphi_{m_k})) \quad (7)$$

The analytical model follows accurately the physics behind the whole process of transmission and direct detection of directly modulated OOFDM signals.

where P_0 is the optical intensity due to the steady driving current value i_0, $P_1(t)$ is the linear optical intensity term (function of $H_{p1}(\omega_k)$), whilst $P_2(t)$ and $P_{11}(t)$ represent the harmonic and intermodulation distortion of the optical intensity modulation (functions of $H_{p2}(\omega_k)$ and $H_{p11}(\omega_k, \omega_1)$, respectively). Finally, the optical modulation frequency indices m_k exp ($j\ \varphi m_k$) in Eq. (7) include both linear and nonlinear effects in the optical phase modulation.

Getting rid of the square root by approximating $\sqrt{1+x} \approx 1 + x/2 - x^2/8$, the fiber transfer function in Eq. (5) can be applied in the frequency domain, and the signal at the fiber output can be determined by calculating its inverse Fourier transform. Neglecting some higher order terms, and using the Graf's theorem for the sum of Bessel functions, one can arrive at the following expression for the photocurrent:

$$I_{ph}(t) =$$

$$\Re \cdot \left(\begin{matrix} T0_{(n_1,n_2,....n_N)} + T1_{(n_1,n_2,....n_N)} + T2_{(n_1,n_2,....n_N)} \\ +T3_{(n_1,n_2,....n_N)} + T4_{(n_1,n_2,....n_N)} + T5_{(n_1,n_2,....n_N)} \end{matrix} \right) \quad (8)$$

$$exp\left(j\left(\Omega_{imp}t + \sum_{k=1}^{N} n_k \left(\varphi_{m_k} + \frac{\pi}{2} \right) \right) \right)$$

$T0$ and $T1$ contain the information component, which can be extracted by setting one of the indices $n_1, n_2,...n_N$ to 1, and the rest to 0, as well as nonlinear distortion due to the laser chirp, the expressions of which are obtained by particularizing the indices $n_1, n_2,...n_N$ such that $\sum_{k=1}^{n}|n_k|>1$. $T2$, $T3$, $T4$ and $T5$ are essentially terms due to nonlinear distortion which stem from the laser nonlinearities ($T2$ and $T3$) and the imbalance caused

by the chromatic dispersion on the optical field ($T4$ and $T5$).

In Fig. 2 the received 32-QAM complex symbols before equalization obtained through the evaluation of with different nonlinear gain coefficient and fiber dispersion values and through the simulation of the IM/DD OOFDM system are shown. We have chosen to show the complex symbols before equalization to demonstrate how accurately the analytical model can follow the physics behind the whole process of transmission and direct detection of directly modulated OOFDM signals.

Although the derived expression for the photocurrent in Eq. (7) offers us a very accurate description of the physical processes which govern the optical transmission, propagation and detection of OOFDM signals in DM/DD systems, we need to derive more intuitive and computationally easy expressions of the linear and nonlinear effects. Such simplification can be carried out by approximating the Bessel functions involved in the photocurrent expression Eq. (8):

$$J_n(x) = \begin{cases} 1, n = 0 \\ \pm\frac{x}{2}, n = \pm 1 \\ 0, otherwise \end{cases} \quad (9)$$

and retaining only the intermodulation distortion products up to the second order. The expression characterizing the linear effects is then reduced to the following equation

$$T0|_{n_r=1} + T1|_{n_r=1} =$$

$$\left(H_{p1}(\Omega_r) \cdot cos\left(-\Omega_r^2 \frac{\beta_2}{2} L \right) + 2jP_0 \cdot H_{\phi1}(\Omega_r) \cdot \quad (10) \right.$$

$$\left. sin\left(-\Omega_r^2 \frac{\beta_2}{2} L \right) \right) \cdot \frac{m}{2} X_r$$

Moreover, the evaluation of the nonlinear distortion is rather direct and still accurate for typical parameter values employed in DM/DD OOFDM systems in short/medium haul links. The resulting nonlinear distortion expressions are:
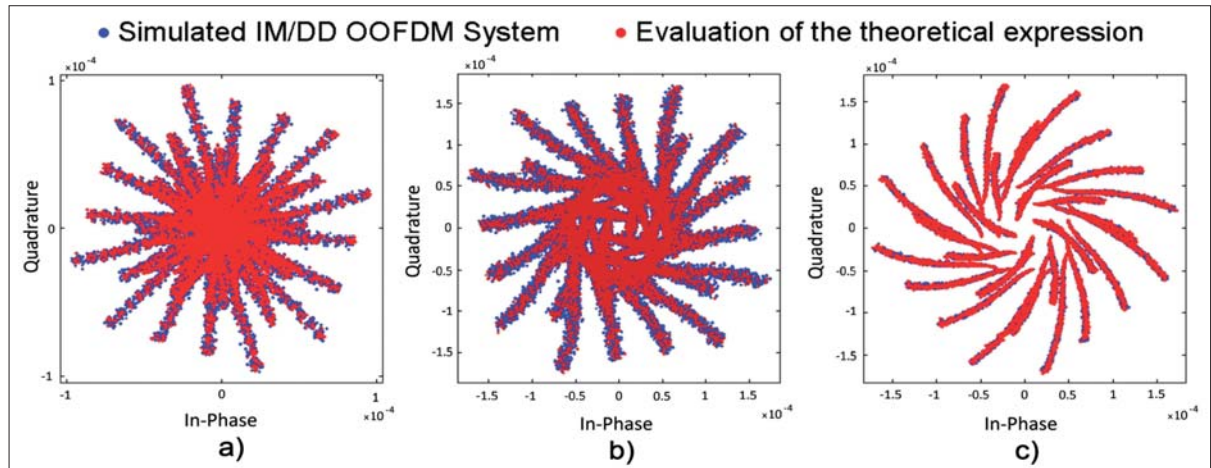

Figure 2. Constellation diagrams obtained through the simulation of the DM/DD OOFDM system and the evaluation of Eq. (7). f_{sam}=11GHz, FS=128, N=55, L=60km, (a) the nonlinear gain coefficient is equal to $3x10^{-24}m^3$; (b) the nonlinear gain coefficient is equal to $3x10^{-23}m^3$; (c) same as (b) but the fiber dispersion is D=-7ps=(nm_km).

$$I_{p,DML}[k] = \sum_{l=1}^{[k/2]-1} H_{p11}(\Omega_l, \Omega_{k-l}) \cdot \cos(\theta_k) \cdot i_l \cdot i_{k-l} \cdot exp\big(j(\varphi_l + \varphi_{k-l})\big) +$$
$$\sum_{l=k+1}^{N} H_{p11}(\Omega_l, -\Omega_{l-k}) \cdot \cos(\theta_k) \cdot i_l \cdot i_{l-k} \cdot exp\big(j(\varphi_l - \varphi_{l-k})\big) \qquad (11)$$

$$I_{\phi,DML}[k] = -2P_0 \sum_{l=1}^{[k/2]-1} H_{\phi11}(\Omega_l, \Omega_{k-l}) \cdot \sin(\theta_k) \cdot i_l \cdot i_{k-l} \cdot exp\big(j(\varphi_l + \varphi_{k-l})\big) +$$
$$-2P_0 \sum_{l=k+1}^{N} H_{\phi11}(\Omega_l, -\Omega_{l-k}) \cdot \sin(\theta_k) \cdot i_l \cdot i_{l-k} \cdot exp\big(j(\varphi_l - \varphi_{l-k})\big) \qquad (12)$$

$$I_{p/\phi,\beta_2}[k] = \sum_{l=1}^{[k/2]-1} \begin{pmatrix} H_{p1}(\Omega_l) \cdot H_{\phi1}(\Omega_{k-l}) \cdot \cos(\theta_l) \cdot \sin(\theta_{k-l}) + \\ H_{p1}(\Omega_{k-l}) \cdot H_{\phi1}(\Omega_l) \cdot \cos(\theta_{k-l}) \cdot \sin(\theta_l) \end{pmatrix} \cdot i_l \cdot i_{k-l} \cdot exp\big(j(\varphi_l + \varphi_{k-l})\big) -$$
$$\sum_{l=k+1}^{N} \begin{pmatrix} H_{p1}(\Omega_l) \cdot H_{\phi1}^*(\Omega_{l-k}) \cdot \cos(\theta_l) \cdot \sin(\theta_{l-k}) + \\ H_{p1}^*(\Omega_{l-k}) \cdot H_{\phi1}(\Omega_l) \cdot \cos(\theta_{k-l}) \cdot \sin(\theta_l) \end{pmatrix} \cdot i_l \cdot i_{l-k} \cdot exp\big(j(\varphi_l - \varphi_{l-k})\big) \qquad (13)$$

$$I_{\phi,\beta_2}[k] = 4P_0 \sum_{l=1}^{[k/2]-1} H_{\phi1}(\Omega_l) \cdot H_{\phi1}(\Omega_{k-l}) \cdot \sin(\theta_l) \cdot \sin(\theta_{k-l}) \cdot i_l \cdot i_{k-l} \cdot exp\big(j(\varphi_l + \varphi_{k-l})\big) -$$
$$4P_0 \sum_{l=k+1}^{N} H_{\phi1}(\Omega_l) \cdot H_{\phi1}^*(\Omega_{l-k}) \cdot \sin(\theta_l) \cdot \sin(\theta_{l-k}) \cdot i_l \cdot i_{l-k} \cdot exp\big(j(\varphi_l - \varphi_{l-k})\big) \qquad (14)$$

$$I_{p,\beta_2}[k] = \frac{1}{P_0} \sum_{l=1}^{[k/2]-1} H_{p1}(\Omega_l) \cdot H_{p1}(\Omega_{k-l}) \cdot \sin(\theta_l) \cdot \sin(\theta_{k-l}) \cdot i_l \cdot i_{k-l} \cdot exp\big(j(\varphi_l + \varphi_{k-l})\big) -$$
$$\frac{1}{P_0} \sum_{l=k+1}^{N} H_{p1}(\Omega_l) \cdot H_{p1}^*(\Omega_{l-k}) \cdot \sin(\theta_l) \cdot \sin(\theta_{l-k}) \cdot i_l \cdot i_{l-k} \cdot exp\big(j(\varphi_l - \varphi_{l-k})\big) \qquad (15)$$

$$I[k] = I_{p,DML}[k] + I_{\phi,DML}[k] + I_{p/\phi,\beta_2}[k] + I_{\phi,\beta_2}[k] + I_{p,\beta_2}[k] \qquad (16)$$

The total nonlinear distortion, I[k], is given by the sum of these terms: and the variance due to nonlinear distortion is calculated as $\sigma_{IMD}^2[k] = \langle |I[k]|^2 \rangle$.

2.2.2. ISI and ICI due to filtering

In order to avoid ISI from the adjacent OFDM symbols and make the linear convolution behave as a circular convolution, cyclic extensions are appended to the original OFDM symbols [2]. Since the transmission information rate is reduced because of the transmission of redundant samples, it is essential to evaluate the penalty due ISI & ICI effects as a function of the number of these redundant samples. The theoretical expressions aimed to evaluate the penalty due to ISI & ICI effects are deduced from similar analysis to those reported in [16,17], but we take into account the correlation between the discrete samples of the generated OFDM signal and we employ the transfer function given by Eq. (10) to include laser intensity and phase modulations as well as the propagation of the signal through the dispersive fiber.

$N_{pre} = \eta_{pre} \cdot FS$ and $N_{preos} = \eta_{pos} \cdot FS$ samples are used as pre- and post-fix for each OFDM symbol. We consider a channel impulse response with a positive tail extending to $T_{sam} \cdot L_+$ and a negative tail extending to $-T_{sam} \cdot L_-$ (L_+ and L_- represent a certain number of samples, and T_{sam} is the sampling period), and we assume that ISI occurs only due to the adjacent OFDM symbols. Apart from ISI, ICI also occurs due to the loss of orthogonality between subcarriers, and the variance characterizing this process has the same value as that due to ISI. The total variance due to ISI & ICI on the k-th subcarrier is given by:

$$\sigma_{ISI}^2[k] + \sigma_{ICI}^2[k] = 2R_x[0] \sum_{q=N_{pre}+1}^{L_+} \big|H_{q,pos_{tail}}[k]\big|^2 + 2R_x[0] \sum_{q=N_{pos}}^{L_--1} \big|H_{q,neg_{tail}}[k]\big|^2$$
$$+ 2 \sum_{\substack{p= \\ N_{pre}+1}}^{L_+} \sum_{\substack{q= \\ N_{pre}+1 \\ q \neq p}}^{L_+} R_x[|p-q|] \cdot e^{j2\pi \cdot k \frac{p-q}{FS}} \cdot H_{p,pos_{tail}}[k] \cdot H_{p,pos_{tail}}^*[k] +$$
$$2 \sum_{\substack{p= \\ N_{pos}}}^{L_--1} \sum_{\substack{q= \\ N_{pos} \\ q \neq p}}^{L_--1} R_x[|p-q|] \cdot e^{-j2\pi \cdot k \frac{p-q}{FS}} \cdot H_{p,neg\_tail}[k] \cdot H_{q,pos\_tail}^*[k] \qquad (16)$$

2.2.3. Clipping of the OFDM signal

After arranging the QAM symbols X_1, X_2,...X_n with Hermitian symmetry at the IFFT input, the signal at the input of the clipping device is given by:

$$x[n] = 2 \cdot Real\left\{\sum_{k=0}^{FS-1} X_k \cdot exp\left(j \cdot 2\pi \cdot k \frac{n}{FS}\right)\right\} \quad (17)$$

As the central limit theorem, for a sufficiently high value of N, $x[n]$ follows a Gaussian distribution with zero mean and variance equal to $2N\sigma_x^2 (\sigma_x^2 = \langle |X|^2 \rangle)$. This means that high peak values of amplitude occur with a small probability and the OFDM signal presents a high peak-to-average power ratio, which is its main drawback.

A simple technique used to limit the random amplitude of the generated OFDM signal is to deliberately clip it, as shown in Fig. 3.

The value of Aclip is an important system parameter in optical OOFDM systems: the smaller its value, the smaller the amplitude excursion of the electrical OFDM signal, and therefore less stringent conditions on the design of electronics in the transceiver and higher optical modulation efficiency, but the higher the distortion introduced by such nonlinear operation. Aclip is usually defined in relation to the clipping level CL, given by $CL = A_{clip}^2/\langle|x[n]|^2$.

Recalling the Bussgang's theorem [18], the clipping operation ouput signal can be expressed as the sum of an undistorted signal part and a noisy term:

$$x_{clip}[n] = \chi \cdot x[n] + n_{\bar{p},clip}[n] \quad (18)$$

where $\chi = 1 - erfc CL/2)$, and $n_{\bar{p},clip}[n]$ is the clipping noise, whose expressions for the autocorrelation and the power spectral density can be found in [19]. In Fig. 4 we compare the normalized power spectral density of the clipping noise for different values of CL and N = 60, being FS = 256.
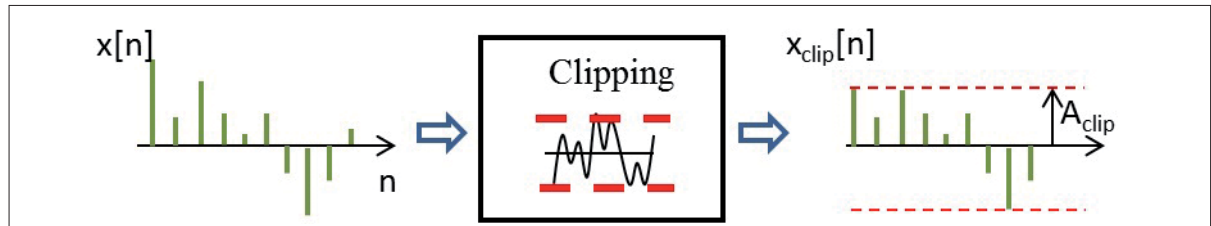
As expected, the smaller the value of CL, higher is the clipping noise introduced, and its spectral density ranges from values around -40dB/Hz for CL = 10dB to values around -20dB/Hz for CL = 5dB. We observe from Fig. 4.4 that comparisons between the PSDs obtained through theory and the simulations are in good agreement.

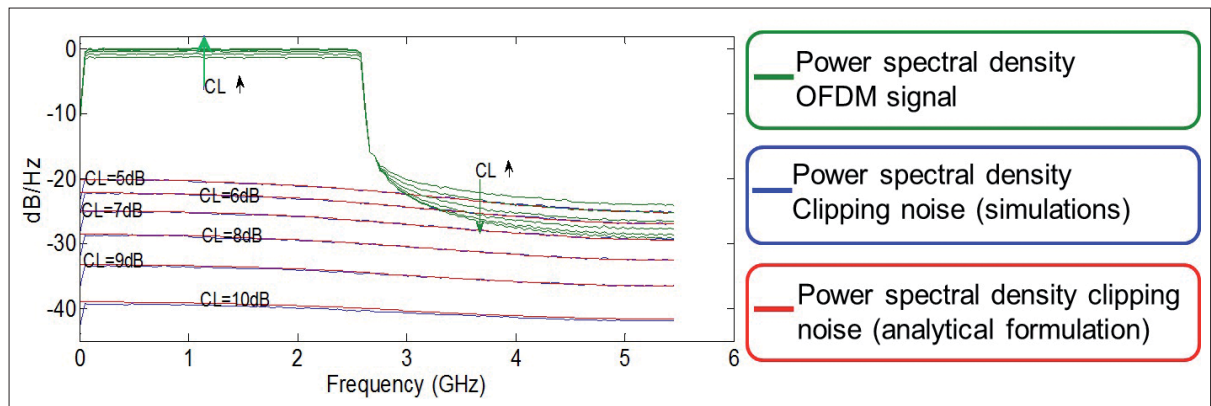The noise variance on the kth subcarrier at the receiver can be calculated as:

$$\sigma_{\bar{p},clip}^2[k] = n_{\bar{p},clip}(e^{j\Omega_k}) \cdot \left|H(e^{j\Omega_k})\right|^2 \Delta\Omega \quad (19)$$

where $H(e^{j\Omega_k})$ is the transfer function from the transmitter IFFT to the receiver FFT, and $n_{\bar{p},clip}(e^{j\Omega_k})$ is the power spectral density of $n_{\bar{p},clip}[n]$.

The spectral estimation of the clipping noise $n_{\bar{p},clip}(e^{j\Omega_k})$ involves a statistical averaging and the clipping noise is assumed to be uniformly distributed with time. However, CL is usually set to a high value and, thus, clipping is a rare event [20]. In order to get a better approach in these situations, we propose to divide the whole clipping process into a finite number of processes, which are given by the union of the OFDM symbols with the same number of clips. Once obtained the power spectral density of the clipping noise with a certain clipping rate i/FS, with $i=0,1,..i_{max}$, that is, $n_{i,clip}(e^{j\Omega_k})$, the variance is of

■ **Figure 3.** Clipping operation.

■ **Figure 4.** Power spectral density of the clipped signal and the clipping noise for FS = 256 and N = 60.

the kth subcarrier at the receiver can be calculated as:

$$\sigma_{i,clip}^2[k] = n_{i,clip}(e^{j\Omega_k}) \cdot \left|H(e^{j\Omega_k})\right|^2 \Delta\Omega \qquad (20)$$

which can be used in a more refined expression of the error probability:

$$Pr(bit\ error) = \sum_{i=0}^{i_{max}} Pr(bit\ error|i\ clips)\,Pr(i\ clips) \quad (21)$$

This approach has demonstrated to provide a more accurate evaluation of the clipping effects than the traditional one based on the direct computation of the power spectral density of the clipping noise [21].

3. Performance evaluation

Due to the unique algorithm used to demultiplex the received OFDM signal through the use of a FFT, the different impairment effects which add to the received complex symbol, $H[k] \cdot X[k]$, can be approximated to a Gaussian distribution [2] provided a sufficiently high number of data subcarriers N is used. Thus, the system performance evaluation can be accomplished through a simple figure of merit which accounts for the power of the undistorted part of the received information signal and the variance of the impairment effects on each subcarrier [8]. In order to calculate the BER of each subcarrier (BER[k]), due to the analytical treatment to study the clipping noise explained in the subsection 2.2.3, a signal-to-noise ratio conditioned to the number of clips i is calculated

$$SNR_{i,clips}[k] = \frac{|H[k]|^2}{\sigma_{S\&t}^2[k] + \sigma_{ISI\&ICI}^2[k] + \sigma_{i,clip}^2[k] + \sigma_{IMD}^2[k]} \quad (19)$$

Once determined $SNR_{i,clips}[k]$, BER[k] with k = 1,…,N is easily determined with the help of BER evaluation formulas [21] and making use of Eq. (21).

The arrows in Fig. 5 indicate at which point the maximum value of transmission information rate is achieved, being 27.63Gbits/s for i_0=46mA, α = 4 and εnl = 1.7×10^{-23}m^3, and 26.606Gbits/s for i_0=78mA, α = 7 and ε_{nl} = 1.7×10^{-23}m^3. From Fig. 5(a) we can observe that the system performance is clearly limited by the laser chirp and the information transmission rate decreases with α, whereas for i_0 = 78mA, a higher value of α is beneficial because of the linear contribution due to the laser chirp, as expressed in Eq. (10). The variation of the achievable information transmission rate with ε_{nl} is due to two counteracting factors: at small values, frequency dips may appear as result of the opposite phases between the two terms in Eq. (10), and at higher values, laser nonlinearity becomes more significant.

4. Applications for system performance enhancement

4.1. Pre-distortion technique
The principle is rather simple and is based on the reconstruction of the interference $I[k]$ with $k = 1,2...N$ and proper substraction at the transmitter. It is assumed that the channel varies at a sufficiently slow speed such that the transmitter is able to track the changes of $I[k]$, with $k = 1,2...N$, through appropriate feedback information from the receiver, which is a reasonable assumption for short/medium IM/DD links. The reconstruction of the interfering term $I[k]$ with $k = 1,2...N$ is based on the ana-

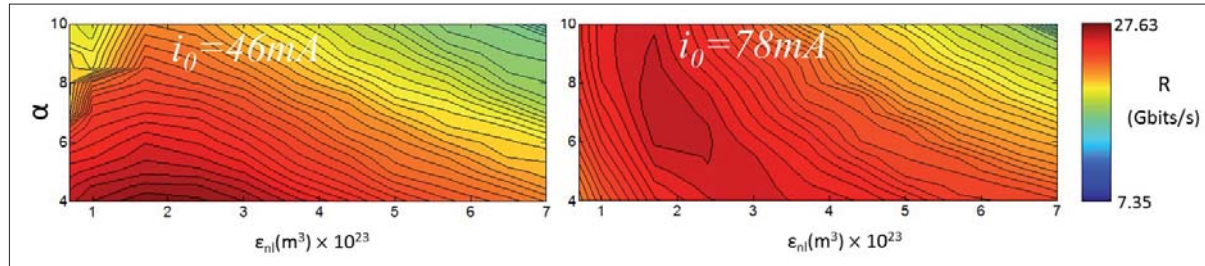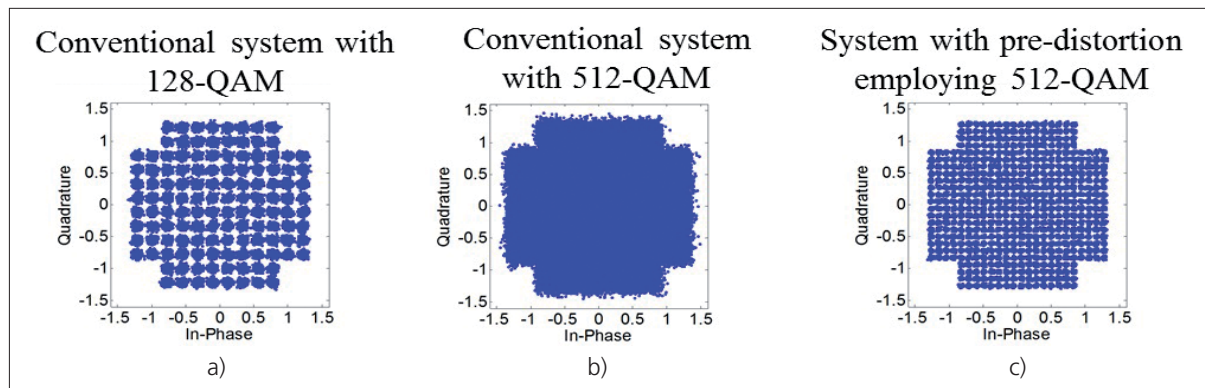**Figure 5.** Information transmission rate for a) i0 = 46mA and b) i_0 = 78mA.

Figure 6. Constellation diagrams of the 62th to 110th subcarriers for L = 40km. a) Conventional DM/DD OOFDM system (128-QAM), b) DM/DD OOFDM system without pre-distortion technique (512-QAM), and c) DM/DD OOFDM system with pre-distortion technique (512-QAM).

lytical model reported in section 2.2.1. Apart from the feedback provided by the receiver, another feedback path is employed at the transmitter in order to identify other magnitudes needed for the reconstruction of $I[k]$, what is done by splitting the laser output signal into two signals by means of an optical power divider.

Denoting as $I_{rec}[k]$ the interference reconstructed at the transmitter, it is divided by the linear transfer function $H[k]$, $k = 1,2...N$. The information complex symbols with the proposed technique turn into:

$$X_{prd}[k] = X[k] - \frac{I_{rec}[k]}{H[k]}, k = 1, \dots N \quad (19)$$

As result of the transmission of $X_{prd}[k]$ instead of $X[k]$, $k = 1,2, \dots N$, we have at the output of the communication system:

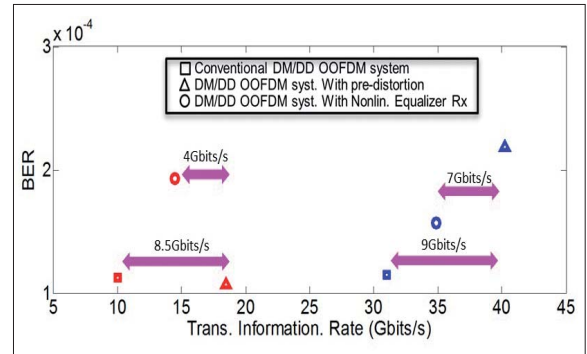$$Y[k] = H[k] \cdot X[k] + \chi[k], k = 1, \dots N \quad (20)$$

where $\chi[k]$ is a difference term due to the transmission of $X_{prd}[k]$ instead of $X[k]$, $k = 1,2, \dots N$ through the non-linear communication system. With this technique, the system performance increases provided that the reconstructed interference $I_{rec}[k]$ is sufficiently close to the actual interference $I[k]$ and the magnitude of the additional nonlinear term $\chi[k]$ is smaller than $I[k]$, which is a reasonable assumption in a communication system using high order QAM modulation formats and the symbols must be weakly impaired in order to assure a certain performance (e.g., $BER_T < 10^{-4}$).

In Fig. 6 we show the constellation diagrams of the 62th-110th subcarriers in order to get a visual impression of the improvement achieved by means of the proposed pre-distortion technique.

The conventional DM/DD OOFDM system employs 128-QAM in the subcarriers ranging from 62 to 110, and the received symbols after equalization are shown in Fig. 6(a). Using this modulation format guarantees that the obtained BER does not exceed considerably the objective $BER_T = 10^{-4}$, situation which would occur if the modulation format order is increased to 512-QAM. The aim of the constellation diagrams Figs. 6(b) and (c) is to show the effects of the proposed pre-distortion technique. Both of them show the constellation diagram for the same subcarriers (62 to 110), using 512-QAM as modulation format, but in Fig. 6(b) the pre-distortion technique is not used at all. It is clear that the quality of the received signal is ruined and it would lead to an unacceptable value of BER_T. The use of the pre-distortion technique, Fig. 6(c), offers us a much clearer constellation diagram, and, similarly to Fig. 6(a), an appropriate quality of the

received symbols is achieved and the value of the obtained BER_T does not increase significantly.

In Fig. 7 we compare the BER obtained through error-counting simulations of the conventional systems, the system with the proposed pre-distortion technique, and the system with the non-linear equalizer proposed in [10].

■ **Figure 7.** Comparison of BER values obtained through error-counting simulations.

We observe from Fig. 7 that the obtained BER values are close to the objective BER = 10^{-4}. As predicted by the simulations with the simplified model, the achieved transmission information rates when the pre-distortion technique is used are considerably higher. With the nonlinear equalizer at the receiver, the transmission information rates are equal to 33.08Gbits/s and 14.49Gbits/s for L=40km and L=100km, respectively. Though the values obtained with the nonlinear equalizer at the receiver are not the result of a so exhaustive system parameter optimization, the values presented in Fig. 5.10 show an intuitively clear issue: a nonlinear equalization at the receiver can improve the quality of the detected signal, but, since the interference reconstruction depend on decisions about the received information signal, the obtained performance will eventually depend on the signal quality of the conventional DM/DD OOFDM system.

4.2. Optical filtering

The optically filtered DM/DD OOFDM system is very similar to that shown in Fig. 1, but with an optical filter inserted into the optical fibre link. The effects of the optical filtering onto the optical signal can be easily taken into account using the well-known digital filtering theory. The impulse response and corresponding transfer function of the optical filter are given by:

$$h_{fil}(t) = \sum_{\kappa=0}^{Ord-1} h_\kappa \cdot \delta(t - \tau_\kappa) \leftrightarrow H_{fil}(\Omega) = \quad (21)$$

$$: \sum_{\kappa=0}^{Ord-1} h_\kappa \, e^{-j \cdot \tau_\kappa \Omega}$$

where Ord is the order of the filter. The field at its output is calculated as

$$E_{fil}(t, z = L) = \sum_{\kappa=0}^{Ord-1} h_\kappa \cdot E(t - \tau_\kappa, z = L) \quad (22)$$

Finally, the photocurrent is calculated as the squared modulus of the field. After a lengthy mathematical manipulation, $I_{ph}(t')$ can be expressed as eq. (23).

From Eq. (23), we can observe that the different spectra components are weighted by the product of the filter coefficients $h_\kappa \cdot h_\varepsilon^*$ and are also affected by the average phase delay $(\tau_\kappa + \tau_\varepsilon)2$. Because of the complexity of the expressions obtained, we have proceeded as in the section 2.2.1 and we have obtained a simplified version which gives reasonable good results. With these simplifications and making use of the transfer function of the optical filter Eq. (21) the expression for the signal information component can be expressed as:

$$
I_{ph}(t) =
$$
$$
\Re \cdot \sum_{\kappa=0}^{Ord-1} \sum_{\varepsilon=0}^{Ord-1} h_\kappa \cdot h_\varepsilon^* \begin{pmatrix} T0_{(n_1,n_2,\ldots n_N)}(\kappa,\varepsilon) + T1_{(n_1,n_2,\ldots n_N)}(\kappa,\varepsilon) + T2_{(n_1,n_2,\ldots n_N)}(\kappa,\varepsilon) \\ +T3_{(n_1,n_2,\ldots n_N)}(\kappa,\varepsilon) + T4_{(n_1,n_2,\ldots n_N)}(\kappa,\varepsilon) + T5_{(n_1,n_2,\ldots n_N)}(\kappa,\varepsilon) \end{pmatrix} \cdot
$$
$$
exp\left(j\left(\Omega_{imp}t + \sum_{k=1}^{N} n_k \left(\frac{\tau_\kappa + \tau_\varepsilon}{2} + \varphi_{m_k} + \frac{\pi}{2}\right)\right)\right)
\tag{23}
$$

$$
T0|_{n_r=1} + T1|_{n_r=1} =
$$
$$
\begin{pmatrix} \frac{H_{fil}^*(0)\cdot H_{fil}(\Omega_r)}{2}\left(H_{p1}(\Omega_r)\cdot e^{-j\Omega_r^2\frac{\beta_2}{2}L} + 2P_0 \cdot H_{\phi1}(\Omega_r)\cdot e^{-j\Omega_r^2\frac{\beta_2}{2}L}\right) + \\ \frac{H_{fil}(0)\cdot H_{fil}^*(\Omega_r)}{2}\left(H_{p1}(\Omega_r)\cdot e^{j\Omega_r^2\frac{\beta_2}{2}L} - 2P_0 \cdot H_{\phi1}(\Omega_r)\cdot e^{j\Omega_r^2\frac{\beta_2}{2}L}\right) \end{pmatrix} \cdot \frac{m}{2} X_r
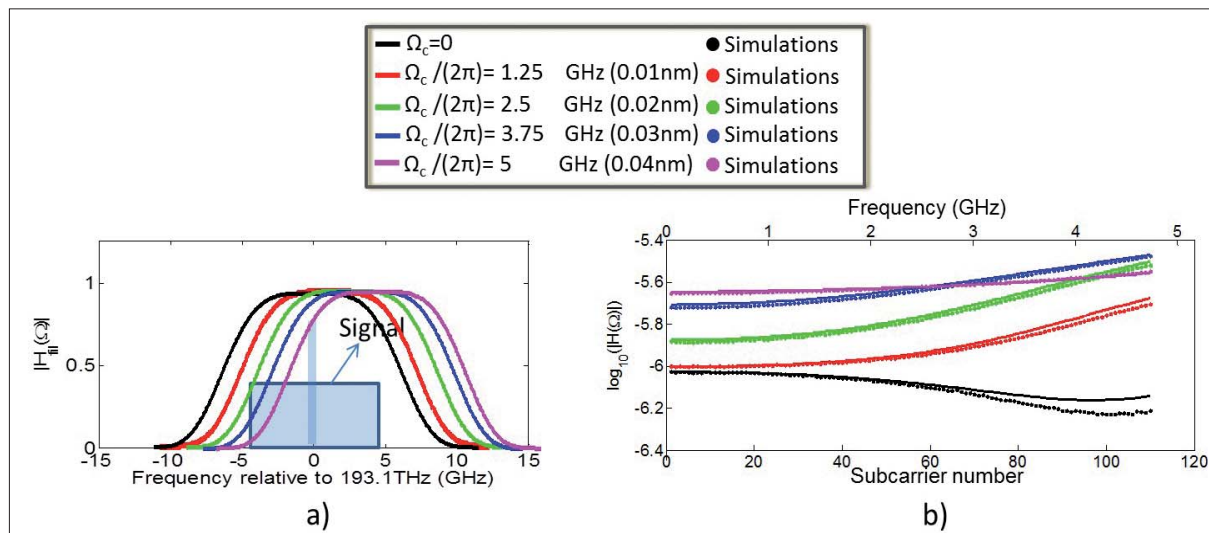\tag{24}
$$

In Fig. 8 an optical superGaussian filter of order 2 and 3-dB bandwidth of 10GHz is used to observe the influence of the central frequency shift with respect to the optical carrier of the information signal.

As Eq. (24) points out, in the case some asymmetry is introduced, information components that otherwise would be counteracted, start to spring up, increasing thus the signal information detected at the receiver and the system, as it is observed in Fig. 8(a) and (b): the increase of the central frequency implies a stronger filtering of the lower sideband, and such asymmetry leads to the increase of the system transfer function plotted in Fig. 8(b).
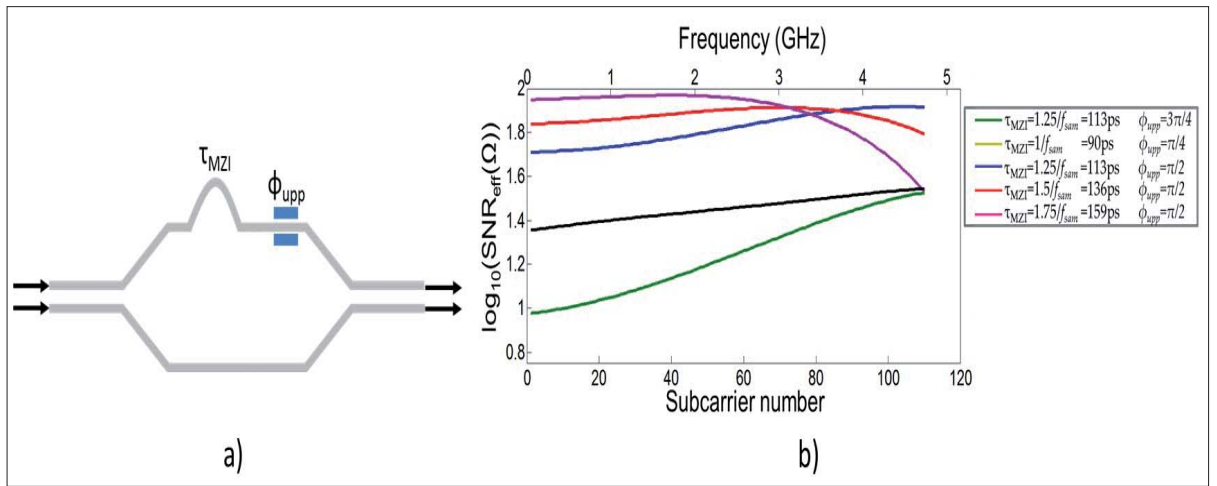
Using the signal-to-noise ratio figure defined in Eq. (19), we can study the expected performance of an optically filtered OOFDM system with different optical filtering architectures. In Fig. 9(b) we show the obtained signal-to-noise ratio obtained for different values of the delay τ_{MZI} and the phase shift ϕ_{upp} of a Mach-Zehnder interferometer filter, shown in Fig. 9(a).

We can see in Fig. 9(b) that with a simple MZI we have been able to get an effective SNR around 19dB, which is obtained when $\phi_{upp}=\pi/2$. This value for the phase shift entails a tradeoff point of the system, mainly determined by the optical carrier attenuation and the degree of imbalance introduced. When the value for ϕ_{upp} is changed to $\pi/4$ or $3\pi/4$ the effective SNR gets worse as a result of a decrease of the system transfer function (Eq. (24)). We can also observe that for $\phi_{upp}=\pi/2$, the delay τ_{MZI} can be varied over a broad range and good values of signal-to-noise ratio are still obtained.

Figure 8. (a) Optical filter transfer function, (b) OOFDM system transfer function with q = 2, $\Delta\Omega_{3dB}/(2\pi) = 10$GHz (0.08nm).

■ Figure 9. (a) Schematic of the Mach-Zehnder interferometer filter, (b) Signal to noise ratio for different values of the delay and phase shift.

Finally, the performance improvement provided by the optical filtering is quantified in terms of power budget. In Fig. 9 we show the BER obtained for different values of the received average optical power. Based on the previous results, we set τ_{MZI} to 136ps and $\phi_{upp}=\pi/2$. Given the importance of the clipping ratio used at the transmitter on the system performance, curves with different values of clipping ratio have been also plotted.

The performance improvement obtained by inserting the optical filter in the OOFDM system is highly dependent on the clipping ratio: when no optical filter is used, a significant power budget improvement can be obtained by reducing the clipping ratio, whilst this reduction results in a more limited improvement in the distortion-limited power budget when an optical filter is used. When no optical filter is used, a received power equals to -15.2dBm is needed to achieve a BER equals to 10^{-3} when CL=13.8dB, whilst a received power equals to -17.6dBm is needed for CL=8dB. When a MZI is used, for which a received power equals to -20.9dBm is needed to obtain a BER equals to 10^{-3} when CL=13.8dB, whilst it is reduced to -22.1dBm when CL=10dB, as it can be observed in Fig. 9(b). Thus, with a MZI as optical filter, we are able to get an improvement equals to 4.5dB compared to the non-optically filtered system.

5. Conclusions

The proposed mathematical treatment has allowed us to include the main signal generation, transmission and detection effects, as well as providing us with a great versatility. After proper validation by comparing the results with those obtained with simulation commercial software, the analytical model has offered us a mathematical description of the linear information signal term and the nonlinear distortion at the receiver-end side, determining jointly to a great extent the obtained system performance of DM/DD OOFDM systems. To the best of our knowledge,

the proposed model represents the most accurate model up to the present day for the accounting of the main effects in DM/DD OOFDM systems. Furthermore, despite of its complexity, it can be conveniently simplified to provide a much more simple description accordingly to the needs of the particular system. A more complete description of real DM/DD OOFDM systems with the consideration of important transceiver design parameters, such as the clipping level, the length of the cyclic extensions and the laser modulation index, has been also derived.

In order to deal with the underlying problem of nonlinear distortion in DM/DD OOFDM system, a novel pre-distortion technique has been proposed based on the previously proposed analytical model. In the proposed scheme, a dedicated receiver extracts and tracks some of the necessary parameters needed to reconstruct the interference terms of the system. Together with the feedback-path from the receiver to the transmitter, the proposed technique is able to achieve great nonlinear distortion reduction ratio values.

Transmission information rates equal to 40Gbits/s and 18.5Gbits/s have been obtained for L=40km and L=100km, respectively, with a BER in the order of 10^{-4}. The employment of QAM modulation formats of higher order to those used in the conventional DM/DD OOFDM system has allowed us to obtain transmission information rate improvements equal to 9Gbits/s and 8.5Gbits/s for L=40km and L=100km, respectively. Furthermore, comparisons of the pre-distortion technique with a previously reported nonlinear mitigation technique based on nonlinear equalization at the receiver-end side have been also carried out, showing that our proposed technique achieves a higher nonlinear distortion cancellation efficiency. As result, our proposed technique outperforms nonlinear equalization at the receiver by several Gbits/s.

Through the development of the corresponding analytical model, we have been able to grasp the foundation

for the improvement obtained when an optical filter is used in a DM/DD OOFDM system. Results obtained have confirmed that optical filtering may be a suitable technique for the improvement of power budget in DM/DD OOFDM systems by a few dBs (4.5dB with a MZI). The analytical formulation obtained for the description of optically filtered DM/DD OOFDM systems has demonstrated to be an useful tool to characterize the system performance through the calculation of the effective signal-to-noise ratio. Its computation has allowed us to explore optimized values for a MZI filter.

To sum up, DM/DD OOFDM systems are suitable option to be employed in dynamical metro/access optical networks, able to provide great spectral efficiencies and versatility. The cost of such systems is also one of its main advantages, compared to other architectures such as externally modulated/directly detected systems or coherently detected systems. The laser chirp impose limitations on the link reach and the achievable transmission information rate, but, as we have seen in this work, DSP and optical signal processing techniques may make a valuable contribution to mitigate their effects. Other disadvantages arising from the nature of the information transmission (it must be conveyed in the optical intensity domain), such as the loss of the information on the phase and polarization of the optical signal make DM/DD systems unflattering compared to their more complex counterparts.

References

[1] W. Shieh and I. Djordjevic, OFDM for Optical Communications, Elsevier/Academic Press, 2009.

[2] J. Armstrong, "OFDM for optical communications," J. Lightw. Technol., vol. 27, no. 3, pp.189–204 2009

[3] E. Hugues-Salas, R. P. Giddings, X. Q. Jin, J. L.Wei, X. Zheng, Y. Hong, C. Shu, and J. M. Tang, "Real-time experimental demonstration of low-cost VCSEL intensity-modulated 11.25Gb/s optical OFDM signal transmission over 25km PON systems," Opt. Express, vol. 19, no. 4, pp. 2979–2988, 2011.

[4] D. Visani, C. Okonkwo, S. Loquai, H. Yang, Y. Shi, H. van de Boom, T. Ditewig, G. Tartarini, B. Schmauss, J. Lee, T. Koonen, and E. Tangdiongga, "Beyond 1Gbit/s transmission over 1 mm diameter plastic optical fiber employing DMT for in-home communication systems," J. Lightw. Technol., vol. 29, no. 4, pp. 622–628, 2011.

[5] N. Cvijetic, D. Qian, and T. Wang, "10Gb/s free-space optical transmission using OFDM," in OFC/NFOEC 2008, paper OThD2.

[6] N. Cvijetic, D. Qian, J. Hu, and T. Wang, "Orthogonal frequency division multiple access PON (OFDMA-PON) for colorless upstream transmission beyond 10 Gb/s," IEEE J. Sel. Areas Commun. 28(6), 781–790 (2010).

[7] X. Q. Jin, E. H-Salas, R. P. Giddings, J. L. Wei, J. Groenewald, and J. M. Tang, "First real-time experimental demonstrations of 11.25Gb/s optical OFDMA PONs with adaptive dynamic bandwidth allocation," Opt. Express, vol. 19, no. 21, pp. 20557–20570, 2011.

[8] E. Vanin, "Performance evaluation of intensity modulated optical OFDM system with digital baseband distortion," Opt. Express, vol. 19, no. 5, pp. 4280–4293, 2011.

[9] C-C. Wei, "Small-signal analysis of OOFDM signal transmission with directly modulated laser and direct detection," Opt. Lett., vol. 36, no. 2, pp. 151–153, 2011.

[10] C-C. Wei, "Analysis and iterative equalization of transient and adiabatic chirp effects in DML-based OFDM transmission systems," Opt. Express, vol. 20, no. 23, pp. 25774–25789, 2012.

[11] Z. Liu, M. A. Violas, and N. B. Carvalho, "Digital predistortion for RSOAs as external modulators in radio over fiber systems," Opt. Express, vol. 19, no. 18, pp. 17641–17646, 2011.

[12] Y. Bao, Z. Li, J. Li, X. Feng, B. Guan, and G. Li, "Nonlinearity mitigation for high-speed optical OFDM transmitters using digital pre-distortion," Opt. Express, vol. 2, no. 6, pp. 7354–7361, 2013.

[13] L.-S. Yan, Y. Wang, B. Zhang, C. Yu, J. McGeehan, L. Paraschis, and A. E. Willner, "Reach extension in 10-Gb/s directly modulated transmission systems using asymmetric and narrowband optical filtering," Opt. Express, vol. 13, no.13, pp. 5106–5115, 2005.

[14] J. L. Wei, C. Sánchez, R. P. Giddings, E. Hugues-Salas, and J. M. Tang, "Significant improvements in optical power budgets of real-time optical OFDM PON systems," Opt. Express, vol. 18, no. 20, pp. 20732–20745, 2010.

[15] G. P. Agrawal and N. K. Dutta, Semiconductor Lasers, Van Nostrand Reinhold, 1993.

[16] W. Henkel, G. Taubock, P. Odling, P. O. Borjesson, and N. Petersson, "The cyclic prefix of OFDM/DMT - an analysis," IEEE Seminar on Broadband Commun., Zurich, Switzerland, 2002.

[17] D. J. F. Barros and J. M. Kahn, "Optimized dispersion compensation using orthogonal frequency-division multiplexing," J. Lightwave Technol. Vol. 26, no. 16, pp. 2889-2898, 2008.

[18] H. E. Rowe, "Memoryless nonlinearities with Gaussian input: Elementary results," Bell Syst. Tech. J., Vol. 61, No. 7, pp. 1519-1525, Sep. 1982.

[19] R. Gross, D. Veeneman, "SNR and spectral properties for a clipped DMT ADSL signal," IEEE Int. Conf. On Comm., Vol. 2, No. 843–847, May 1994.

[20] C. Sánchez, J. L. Wei, B. Ortega, J. Capmany, "Comprehensive impairment and performance description of directly modulated/detected OOFDM systems," J. Lightw. Technol., vol. 3, no. 20, pp. 3277–3288, 2013.

[21] J. G. Proakis, Digital Communications, 4th ed. McGrawHill, 2000.

Biographies

Dr. Christian Sánchez received the Telecommunication Engineer bachelor's degree in 2008, the M.Sc. degree in 2010 and PhD in 2014 from the Universidad Politecnica de Valencia. Since March 2008, he was working toward the Ph.D. degree in the Optical and Quantum Communications Group. He has been involved in the european project ALPHA and the national project NETWON. In 2010, he was a Guest Researcher at the Bangor University, under the supervision of Prof. J. Tang. He is currently at the Aston University, Birmingham, as post-doctoral research fellow, studying digital signal processing techniques to be employed in optical communication systems with spatial division multiplexing. His main research interests include optical fiber communications, advanced optical modulation formats and signal processing techniques. He serves as reviewer for journals of his field, such as Photonics Technology Letters, Journal Lightwave of Technology, Optics Letters and Optics Express.

Dr. Beatriz Ortega was born in Valencia, Spain, in 1972. She received the M.Sc. degree in physics in 1995 from the Universidad de Valencia, and the Ph.D. in Telecommunications Engineering in 1999 from the Universidad Politécnica de Valencia. She joined the Departamento de Comunicaciones at the Universidad Politécnica de Valencia in 1996, where she was engaged to the Optical Communications Group and her research was mainly done in the field of fibre gratings. From 1997 to 1998, she joined the Optoelectronics Research Centre, at the University of Southampton (United Kingdom), where she was involved in several projects developing new add-drop filters or twin-core fibre-based filters. Since 1999 she is an Associate Lecturer at the Telecommunications Engineering Faculty in the Universidad Politécnica de Valencia. She has published more than 100 papers and conference contributions in fibre Bragg gratings, microwave photonics and optical networks. She has participated in the European Networks of Excellence IST-NEFERTITI, IST-EPIXNET, and IST-EPHOTON/ONE and she has also been involved in several EU funded projects such as IST-LABELS, IST-GLAMOROUS, IST-OFFSOHO and IST-ALPHA project. Currently she is leading the NEWTON national project, where her main research is focused on advanced modulation techniques in optical systems.

José Capmany obtained the M.Sc. degrees in Telecommunications Engineering and Physics from Universidad Politecnica de Madrid (UPM) and UNED respectively. He holds a Ph.D. in Telecommunications Engineering from UPM and a Ph.D. in Physics from the Universidad de Vigo. In 1991 he moved to the Universidad Politecnica de Valencia (UPVLC) where he has been a full Professor in Photonics and Optical Communications since 1996. In 2002 he was appointed Director of the Institute Of Telecommunications and Multimedia (iTEAM) at UPVLC. He has been engaged in many research areas within the field of photonics during the last 25 years including Microwave Photonics, Integrated Optics, Fiber Bragg Grating design and fabrication, Optical Networks and, most recently Quantum Information systems. He has published over 375 papers in scientific journals and confererences. He is a Fellow of the Institute of Electrical and Electronic Engineers (IEEE) and the Optical Society of America (OSA). In 2012, he was awarded with the Rey Jaime I on New Technologies.